Accuracy of the Domain Material Derivative Approach to Shape Design Sensitivities

R. J. Yang* and M. E. Botkin†
General Motors Research Laboratories, Warren, Michigan

Numerical accuracy for the boundary and domain methods of the material derivative approach to shape design sensitivities is investigated through the use of mesh refinement. The results show that the domain method is generally more accurate than the boundary method using the finite-element technique. It is also shown that the domain method is equivalent, under certain assumptions, to the direct differentiation approach that evaluates sensitivities by direct-differentiating the implicit discretized equilibrium equation, not only theoretically but also numerically.

Introduction

Haug and Choi et al.[1-4] developed a unified theory of structural design sensitivity analysis for linear elastic structures, using a variational formulation of the structural state equations. Unlike the direct differentiation approach that obtains the sensitivities by direct-differentiating the implicit discretized equilibrium equation, this theory allows one to take the total derivative, or material derivative, of the variational state equation and to use an adjoint variable technique for design sensitivity analysis. The main attraction of this approach is that it allows one to compute analytically the derivatives of structural performances. No discretization approximations are involved during the derivation, and a step size need not be specified in the calculation. However, the formulation requires evaluating accurate stress quantities on the boundaries that are often difficult to obtain.

Accuracy of the shape design sensitivity theory was studied in Ref. 5 through the equilibrium condition for different types of finite elements. However, a systematic study through the refinement of the finite-element mesh was still not found in the literature.

To improve the accuracy of shape design sensitivities, Choi et al.[6] proposed a new domain method that transforms the boundary integrals into domain integrals and therefore is less influenced by the inaccurate boundary stress evaluation. This method takes advantage of the averaging nature of the finite-element method and is found to be more accurate than the boundary approach that evaluates the derivatives using boundary information only.[1-3] However, a velocity field for the physical domain needs to be defined. The necessity of defining the domain velocity may indicate that this method is closely related to the direct differentiation approach that also requires knowledge about the domain change for differentiation of the elemental stiffness matrix.[7]

In a previous paper,[8] the boundary integral formulation was shown to be equivalent to the direct differentiation approach, theoretically. In this paper, the domain method is shown to be equivalent to the direct differentiation method, both in theoretical and numerical aspects. The accuracy of the design sensitivity is studied through finite-element mesh refinement for a cantilever thin plate. Results of the domain and boundary methods for the material derivative approach and the direct differentiation approach are shown and compared. A more realistic automotive arm problem is used to reassure the equivalence of the domain and direct approaches.

Received Nov. 18, 1986; revision received April 8, 1987.

*Senior Research Engineer, Engineering Mechanics Department.
†Senior Staff Research Engineer, Engineering Mechanics Department.

Shape Design Sensitivity Analysis

Two approaches for shape design sensitivity analysis are found in the literature. One is the well-known direct differentiation approach and the other is the variational or material derivative approach. Detailed information for these two approaches is available in Refs. 4, 7, and 8. Only a brief background is provided here.

For the direct differentiation approach, the displacement sensitivity is obtained by differentiating the discretized structural system of equations

$$Kz = F \tag{1}$$

By assuming that the force vector F is independent of design, we obtain

$$\frac{\partial z}{\partial b_i} = -K^{-1}\frac{\partial K}{\partial b_i}z \tag{2}$$

where K is the global stiffness matrix, z is the displacement vector, and b_i is the design variable.

The variational design sensitivity theory uses the material derivative concept of continuum mechanics and an adjoint variable method to obtain computable expressions for the effect of shape variation on the functionals arising in the shape design problem. The variation of the displacement functional ψ with respect to shape change is derived by differentiating the variational equilibrium equation and employing the adjoint variable method to obtain[1-4]

$$\delta\psi = \int_\Gamma \sigma^{ij}(z)\varepsilon^{ij}(\lambda)V_k n_k \mathrm{d}\Gamma \tag{3}$$

where ψ is defined by

$$\psi = \int_\Omega z\delta(x-\bar{x})\mathrm{d}\Omega \tag{4}$$

in which $\bar{x}$ is the point of interest, δ the Dirac-measure at zero, Ω the physical domain, σ^{ij} and ε^{ij} the stress and strain tensors, respectively, V the design perturbation and also velocity, and n_k the unit normal vector of moving boundary Γ. (The Einstein summation convention for a repeated index is used throughout this paper.) The vectors z and λ are the displacement vectors for state and adjoint equations, respectively, that can be ex-

pressed as follows:

$$\int_\Omega \sigma^{ij}(z)\varepsilon^{ij}(\bar{z})\mathrm{d}\Omega = \int_{\Gamma^2} T_i\bar{z}_i\mathrm{d}\Gamma \tag{5}$$

$$\int_\Omega \sigma^{ij}(\lambda)\varepsilon^{ij}(\bar{\lambda})\mathrm{d}\Omega = \int_\Omega \delta(x-\bar{x})\bar{\lambda}\mathrm{d}\Omega \tag{6}$$

where T_i is a traction vector, Γ^2 a loaded boundary, and the overbar indicates the virtual displacements that satisfy the kinematically admissible displacement field.

To obtain Eq. (3), the traction vector T_i, the kinematically constrained boundary, and the loaded boundary are assumed to be fixed during the design process, i.e., they are independent of design. Note that the variation of the displacement functional of Eq. (3) is only affected by the normal movement of the boundary of the physical domain.

Physically, the adjoint equation of Eq. (6) is interpreted by applying a unit load at the point $\bar{x}$, where the displacement sensitivity is of interest. In Eq. (3), one sees that only the boundary stress information is needed for evaluating the variation of the displacement functional. Unfortunately, finite-element analysis usually does not provide high-quality stress results, especially on the boundary. It has been shown that better finite-element results give better design sensitivity estimates by examining the equilibrium equations for different finite elements.[5]

Domain Method

The basic idea of the domain integral method is to take advantage of the averaging nature of the finite-element method, instead of evaluating the less accurate stresses on the boundary. Since the finite-element method is well known to provide better solutions inside the finite element, the domain method has the advantage of predicting better sensitivities.

Applying the same procedure as in obtaining Eq. (3) with the domain method, the first variation of the displacement constraint functional of Eq. (4) is obtained as[4,6]

$$\delta\psi = \int_\Omega [\sigma^{ij}(\lambda)z_{i,k}V_{k,j} + \sigma^{ij}(z)\lambda_{i,k}V_{k,j} - \sigma^{ij}(z)\varepsilon^{ij}(\lambda)V_{k,k}]\mathrm{d}\Omega \tag{7}$$

One should note that Eq. (7) is more general than Eq. (3), since only the loaded boundary is assumed to be fixed, whereas both loaded and kinematically constrained boundaries are assumed to be unchanged in Eq. (3). The kinematically constrained boundary and interface boundary terms appear when the divergence theorem is used to transform the domain integral to the boundary integral. It was shown in Ref. 6 that for an interface or builtup structure problem, this method simplifies the formulation and avoids specifying tedious interface conditions and provides increased accuracy for the shape design sensitivities.

To acquire a better understanding of Eq. (7), each term will be examined individually. First, since the stress tensor σ^{ij} is symmetric, the first term of Eq. (7) is divided into two parts and then integrated by parts to obtain

$$\begin{aligned}\int_\Omega \sigma^{ij}(\lambda)z_{i,k}V_{k,j}\mathrm{d}\Omega &= \int_\Omega \sigma^{ij}(\lambda)\frac{1}{2}(z_{i,k}V_{k,j} + z_{j,k}V_{k,i})\mathrm{d}\Omega \\ &= \int_\Gamma \sigma^{ij}(\lambda)\frac{1}{2}(z_{i,k}V_k n_j + z_{j,k}V_k n_i)\mathrm{d}\Gamma \\ &\quad - \int_\Omega \sigma^{ij}(\lambda)\frac{1}{2}(z_{i,kj} + z_{j,ki})V_k\mathrm{d}\Omega\end{aligned} \tag{8}$$

By assuming that only the free boundary is varied, the first term of Eq. (8) disappears, since the traction vector is zero, i.e., $\sigma^{ij}(\lambda)n_j = \sigma^{ij}(\lambda)n_i = 0$. The second term of Eq. (8) then can be further modified to

$$\begin{aligned}\int_\Omega \sigma^{ij}(\lambda)\frac{1}{2}(z_{i,kj} + z_{j,ki})V_k\mathrm{d}\Omega &= \int_\Omega \sigma^{ij}(\lambda)\frac{1}{2}(z_{i,jk} + z_{j,ik})V_k\mathrm{d}\Omega \\ &= \int_\Omega \sigma^{ij}(\lambda)\varepsilon^{ij}_{,k}(z)V_k\mathrm{d}\Omega\end{aligned} \tag{9}$$

where the velocity V_k can be parameterized as $(\partial x_k/\partial b_i)\delta b_i$, in which x_k is the position vector and b_i is the design variable. Since all the integrals are linear in design, one can eliminate δb_i or choose the value as a unit number. By interpreting the adjoint variable λ as the inverse of the reduced stiffness matrix K if all the displacement sensitivities are desired, Eq. (9) is discretized, using the finite-element formulation, as[8]

$$\begin{aligned}\int_\Omega \sigma^{ij}(\lambda)\varepsilon^{ij}_{,k}(z)V_k\mathrm{d}\Omega &= K^{-1}\sum_1^{N_e}\int_{\Omega_e} B^T D B_{,k}\frac{\partial x_k}{\partial b_i}z\,\mathrm{d}\Omega \\ &= K^{-1}\sum_1^{N_e}\int_{\Omega_e} B^T D B_i' z\,\mathrm{d}\Omega\end{aligned} \tag{10}$$

where the subscript i with a prime superscript indicates the derivative with respect to the *ith* design variable. K, D, and B represent the stiffness, elasticity, and strain recovery matrices, respectively. The stress-displacement and strain-displacement relationships are employed in obtaining Eq. (10), which are defined in the following:

$$\sigma^{ij}(\lambda) = DB\lambda \qquad \varepsilon^{ij}(z) = Bz \tag{11}$$

Finally, the first term of Eq. (7) is written as

$$\int_\Omega [\sigma^{ij}(\lambda)z_{i,k}V_{k,j}]\mathrm{d}\Omega = -K^{-1}\sum_1^{N_e}\int_{\Omega_e} B^T D B_i' z\,\mathrm{d}\Omega \tag{12}$$

The second term of Eq. (7) can also be derived in the same way to obtain a similar expression as in Eq. (12) as

$$\int_\Omega [\sigma^{ij}(z)\lambda_{i,k}V_{k,j}]\mathrm{d}\Omega = -K^{-1}\sum_1^{N_e}\int_{\Omega_e} B_i^{T\prime} D B z\,\mathrm{d}\Omega \tag{13}$$

If we substitute Eqs. (12) and (13) into Eq. (7), the following expressions are obtained:

$$\begin{aligned}\delta\psi &= \frac{\partial z}{\partial b_i} \\ &= \int_\Omega [\sigma^{ij}(\lambda)z_{i,k}V_{k,j} + \sigma^{ij}(z)\lambda_{i,k}V_{k,j} - \sigma^{ij}(z)\varepsilon^{ij}(\lambda)V_{k,k}]\mathrm{d}\Omega \\ &= -K^{-1}\sum_1^{N_e}\int_{\Omega_e} B^T D B_i' z + B_i^{T\prime} D B z + B^T D B z V_{k,k}\mathrm{d}\Omega \\ &= -K^{-1}\sum_1^{N_e}\left(\int_{\Omega_e} B^T D B_i' + B_i^{T\prime} D B + B^T D B V_{k,k}\mathrm{d}\Omega\right) z \\ &= -K^{-1}\left[\sum_1^{N_e}\int_{-1}^{+1}\int_{-1}^{+1}\int_{-1}^{+1}(B^T D B_i' + B_i^{T\prime} D B \right. \\ &\quad \left. + B^T D B V_{k,k})|J|\mathrm{d}\xi\,\mathrm{d}\eta\,\mathrm{d}\zeta\right] z\end{aligned} \tag{14}$$

where $|J|$ is the determinant of the Jacobian matrix J that transforms the undeformed configuration into the natural coordinate system. The constraint functional change $\delta\psi$ is equal to $\partial z/\partial b_i$, since all displacement sensitivities are calculated and the design change δb_i is chosen as a unit number.

For the direct differentiation approach of Eq. (2), the derivative of the global stiffness matrix can be evaluated at the elemental level, i.e.,

$$\frac{\partial z}{\partial b_i} = -K^{-1}\frac{\partial K}{\partial b_i}z$$

$$= -K^{-1}\left(\sum_{1}^{N_e} K_i^{e\prime}\right) z \tag{15}$$

where $K_i^{e\prime}$ is calculated numerically in natural coordinates as[7]

$$K_i^{e\prime} = \int_{-1}^{+1}\int_{-1}^{+1}\int_{-1}^{+1} (B_i^{T\prime} DB|J| + B_i^T DB'|J| + B^T DB|J|_i')\,d\xi\,d\eta\,d\zeta \tag{16}$$

Comparing Eqs. (14) and (15), one sees that both are equivalent if the following expression is valid:

$$|J|_i' = |J|V_{k,k} \tag{17}$$

To prove Eq. (17) is true, one should notice that the determinant of the Jacobian can be separated into two parts. The first contribution is from the deformed to undeformed configuration, denoted by $|J|_d$, that depends on design. The other is the contribution of transformation from the undeformed global to local or natural configurations, denoted by $|J|$, that is independent of design. The relationship is expressed in the following form:

$$|J|_\tau = |J|_d|J| \tag{18}$$

where τ denotes the deformed configuration. Differentiating Eq. (18) with respect to design, one obtains

$$|J|_\tau' = |J|_d'|J| \tag{19}$$

It was shown in Ref. 4 that $|J|_d' = V_{k,k}$ at $\tau = 0$, if the design change is assumed to be equal to a unit vector. Thus, Eq. (19) is identical to the form of Eq. (17), and the equivalence of Eqs. (14) and (15) is proved.

Another way to prove the validity of Eq. (17) is to conduct the differentiation directly by the definition of the Jacobian. Consider a two-dimensional case as an example; the right side of Eq. (17) is obtained as

$$\begin{aligned} |J|V_{k,k} &= \left(\frac{\partial x}{\partial \xi}\frac{\partial y}{\partial \eta} - \frac{\partial x}{\partial \eta}\frac{\partial y}{\partial \xi}\right)\left(\frac{\partial V_x}{\partial x} + \frac{\partial V_y}{\partial y}\right) \\ &= \frac{\partial y}{\partial \eta}\frac{\partial V_x}{\partial \xi} + \frac{\partial x}{\partial \xi}\frac{\partial V_y}{\partial \eta} - \frac{\partial y}{\partial \xi}\frac{\partial V_x}{\partial \eta} - \frac{\partial x}{\partial \eta}\frac{\partial V_y}{\partial \xi} \end{aligned} \tag{20}$$

where the velocity V_x and V_y are defined as

$$V_x = \frac{\partial x}{\partial b_i} \qquad V_y = \frac{\partial y}{\partial b_i} \tag{21}$$

If we substitute Eq. (21) into Eq. (20), the following expression is obtained:

$$\begin{aligned} |J|V_{k,k} &= \frac{\partial}{\partial b_i}\left(\frac{\partial x}{\partial \xi}\frac{\partial y}{\partial \eta} - \frac{\partial y}{\partial \xi}\frac{\partial x}{\partial \eta}\right) \\ &= |J|_i' \end{aligned} \tag{22}$$

This simple calculation also verifies that the relationship of Eq. (17) is valid. Note that the design change δb_i is assumed to be unity in Eq. (17).

Numerical Verification and Comparison

In this section, the equivalence of the domain method and the direct differentiation is verified through two examples. The accuracy of design sensitivities for a thin plate is examined and compared through the refinement of the finite-element mesh. A more realistic automotive torque arm reassures the theoretical findings.

Two-Dimensional Thin Plate

A simple two-dimensional thin plate is considered as an example. The finite-element configuration, dimensions, material properties, loading condition, and design variable are shown in Fig. 1. Design variable b is chosen to move the upper-traction free boundary. The load of 100 lb is applied parabolically at the right of the plate.

An eight-noded two-dimensional plane stress isoparametric element is employed for analysis. The boundary stresses and strains that appear in Eq. (3) are computed by extrapolating linearly from the stresses at Gauss points, where the optimal or the best approximate stresses are located. Numerical results for design sensitivity of point A in the Y direction for 1×1, 2×2, 3×3, 4×4, 5×5, and 6×6 meshes are shown in Table 1.

In Table 1, column 1 represents different finite-element meshes and column 2 the displacement of point A in the Y direction for the initial design b. Columns 3 and 4 represent the displacement sensitivities at point A of Fig. 1, using the boundary method (BM) of Eq. (3) and the domain integral (DM) of Eq. (7), respectively, for different meshes. Column 5 lists the results using the direct differentiation approach (DDA) of Eq. (2). The derivative of the global stiffness matrix is carried out by differentiating analytically the element stiffness matrix.

Figure 2 shows the same results as in Table 1. From Fig. 2 and Table 1, one observes that the displacements and the sensitivities for the direct approach do not change much after 3×3 finite-element mesh. However, the design sensitivity for the boundary method of the variational approach is still increasing at the limit of mesh refinement. This implies that the boundary method is more sensitive to the finite-element results, although it provides the analytical formulation for sensitivities. And one concludes that the boundary method of the variational approach tends to yield better gradient estimates, once a more accurate analysis is used and better boundary stresses are obtained. The same conclusion is also found in Refs. 5 and 8.

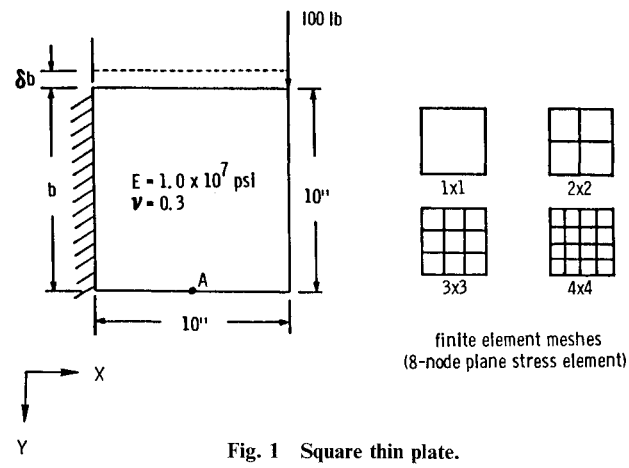

Fig. 1 Square thin plate.

Table 1 Comparison of design sensitivity accuracy

		BM	DM	DDA
Mesh	Displacement, in.	dv/db	dv/db	dv/db
1 × 1	2.495E-5	−4.196E-6	−4.843E-6	−5.248E-6
2 × 2	2.760E-5	−4.518E-6	−5.167E-6	−5.235E-6
3 × 3	2.841E-5	−4.856E-6	−5.369E-6	−5.375E-6
4 × 4	2.845E-5	−4.995E-6	−5.391E-6	−5.394E-6
5 × 5	2.854E-5	−5.093E-6	−5.412E-6	−5.413E-6
6 × 6	2.856E-5	−5.158E-6	−5.425E-6	−5.426E-6

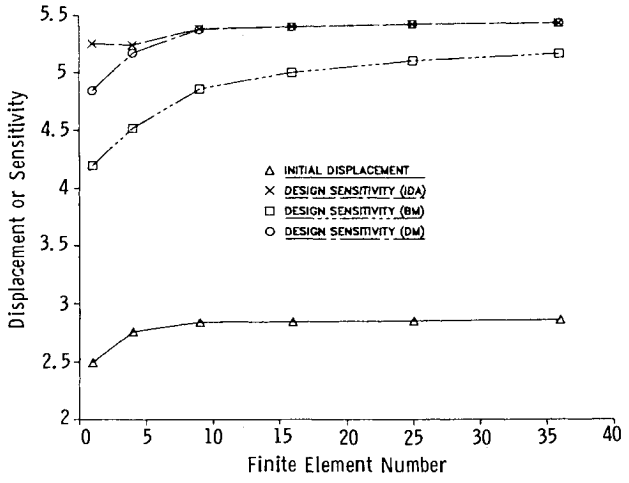

Fig. 2 Accuracy of design sensitivity.

Comparing column 4 with 5, one sees that the domain method results are very close to those obtained from the analytical direct differentiation approach. A clearer interpretation can be observed in Fig. 2, which plots the displacement and displacement sensitivity versus finite-element mesh size. This numerical agreement verifies the equivalence of the two approaches.

In Ref. 8, the boundary method was shown to be theoretically equivalent to the direct approach; however, they yield slightly different results numerically as is also shown in Table 1 and Fig. 2. The difference results from different numerical schemes for these two approaches, i.e., one uses the boundary, and the other the domain information. If consistent numerical schemes are used as for the domain method and the direct approach in this paper, they are shown to be equivalent, not only theoretically but also numerically.

The disadvantage of the domain method is its computational aspects. Numerical evaluation of Eq. (7) is more complicated than evaluation of Eq. (3), because Eq. (7) requires integration over the entire domain, whereas Eq. (3) requires integration only over the variable boundary. In addition, a velocity field that satisfies regularity properties must be defined in the domain. The choice of velocity for the physical domain is more difficult than that for the variable boundary. Although a boundary-layer scheme[9] and a displacementlike velocity field[10] were proposed to alleviate these problems, the domain method still requires more analyst and computational efforts.

Automotive Torque Arm

An automotive rear suspension torque arm studied in Ref. 8 is analyzed in this section, with the geometry, loading conditions, and material properties shown in Fig. 3. For simplicity, a single, nonsymmetric, in-plane static load and plane stress are considered. Zero displacement constraints are applied around the larger hole on the right, in order to simulate attachment to a solid rear axle. Thickness is kept constant at 0.3 cm. The shapes of Γ_1, both upper and lower portions, are to be determined through the optimization process. The other boundary segments are kept fixed.

A spline function that has two continuous derivatives everywhere and has characteristics of global smoothness is employed. Design variables are the distances between the central line and boundary points, shown in Fig. 4. Upper and lower portions of the boundary each have seven design variables. Detailed spline-represented boundary parameterization can be found in Ref. 5.

The finite-element model, illustrated in Fig. 4, includes 204 elements, 707 nodal points, and 1342 degrees of freedom. The

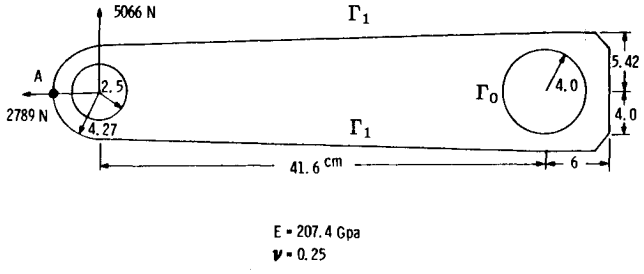

Fig. 3 Automotive torque arm.

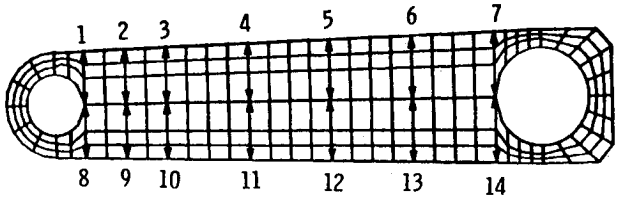

Fig. 4 Design variables and finite element of torque arm.

design sensitivity for vertical displacement of the left end (point A) is computed, using boundary, domain, and direct differentiation methods. The extrapolation strategy for boundary stresses is employed in this case. Results by varying each design variable of the upper boundary by 0.1%; i.e., from 1 to 7, are shown in Table 2.

One observes that in Table 2, the percent errors for the domain (column 4) and direct approaches (column 5), compared to the differences from two finite-element analyses in column 2, are generally very small. Both methods yield comparable and excellent results that reassure the equivalence of these two approaches theoretically and numerically. Column 3 shows the error percentages for the boundary method. As expected, they are the worst among these three methods, since accurate boundary stresses are difficult to obtain in finite-element analysis. One may notice that the percent of errors in Table 2 is different from that in Ref. 8. It is 28.1% in this paper, compared to 3.2% in Ref. 8. The different results are caused by the different boundary parameterizations. In Ref. 8, the velocity or design change used the global information from spline function representation.[5] On the other hand, in this paper only local information is used, i.e., the interior velocity is interpolated by elemental nodal velocities that are exact. Apparently, the boundary method is very sensitive to the boundary representation and the domain-type method (variational or direct) is more forgiving than the boundary method.

Table 2 Percent of error in displacement sensitivities

		BM	DM	DDA
Variable	Δv, cm	Error, %	Error, %	Error, %
1	−7.527E-6	28.1	0.2	0.0
2	−2.524E-6	14.3	0.8	4.1
3	−1.583E-5	14.4	0.2	0.9
4	−4.061E-5	13.9	0.1	0.5
5	−6.719E-5	14.3	0.2	0.4
6	−1.040E-4	13.3	0.1	0.3
7	−8.319E-5	27.6	0.2	0.3

Summary

It is shown that accurate finite-element analysis results in accurate design sensitivities. For the boundary method of the material derivative approach to shape design sensitivities, the accuracy of the finite-element is more crucial, since the finite-element method usually does not give accurate stresses on the boundary.

The domain method is generally more accurate than the boundary method in the material derivative approach for evaluating the design sensitivities; however, a velocity field for the physical domain needs to be defined. The necessity of defining a domain velocity field and integrating the domain integral instead of the boundary integral, as in the boundary method, requires both more analyst and computational time.

It is also shown that the domain method is equivalent, under certain assumptions, to the direct differentiation approach not only theoretically but also numerically. The numerical equivalence is valid only if the numerical methods used for both approaches are consistent.

References

[1]Haug, E. J., Choi, K. K., Hou, J. W., and Yoo, Y. M., "A Variational Method for Shape Optimal Design of Elastic Structures," in *New Directions in Optimum Structural Design*, edited by E. Atrek, R. H. Gallagher, K. M. Ragsdell, and O. C. Zienkiewicz, Wiley, New York, 1984.

[2]Choi, K. K. and Haug, E. J., "Shape Design Sensitivity Analysis of Elastic Structures," *Journal of Structural Mechanics*, Vol. 11, No. 2, 1983, pp. 231–269.

[3]Choi, K. K., "Shape Design Sensitivity Analysis of Displacement and Stress Constraints," *Journal of Structural Mechanics*, Vol. 13, No. 1, 1985, pp. 27–41.

[4]Haug, E. J., Choi, K. K., and Komkov, V., *Design Sensitivity Analysis of Structural Systems*, Academic Press, Orlando, FL, 1986.

[5]Yang, R. J. and Choi, K. K., "Accuracy of Finite Element Based Shape Design Sensitivity Analysis," *Journal of Structural Mechanics*, Vol. 13, No. 2, 1985, pp. 223–239.

[6]Choi, K. K. and Seong, H. G., "A Domain Method for Shape Design Sensitivity Analysis of Built-Up Structures," *Computer Methods in Applied Mechanics and Engineering*, Vol. 57, No. 1, 1986, pp. 1–16.

[7]Ramakrishnan, C. V. and Francavilla, A., "Structural Shape Optimization Using Penalty Functions," *Journal of Structural Mechanics*, Vol. 3, No. 4, 1974–1975, pp. 403–422.

[8]Yang, R. J. and Botkin, M. E., "Comparison Between the Variational and Implicit Differentiation Approaches to Shape Design Sensitivities," *AIAA Journal*, Vol. 24, June 1986, pp. 1027–1032.

[9]Haug, E. J. and Choi, K. K., "Material Derivative Methods for Shape Design Sensitivity Analysis," in *The Optimum Shape: Automated Structural Design*, edited by J. A. Bennett and M. E. Botkin, Plenum, New York, 1986.

[10]Choi, K. K. and Seong, H. G., "A Numerical Method for Shape Design Sensitivity Analysis and Optimization of Built-Up Structures," in *The Optimum Shape: Automated Structural Design*, edited by J. A. Bennett and M. E. Botkin, Plenum, New York, 1986.